Journal of Ceramic Processing Research. Vol. 18, No. 12, pp. 854~857 (2017)

J O U R N A L O F
Ceramic Processing Research

Fabrication of symmetrical $La_{0.7}Ca_{0.3}Cr_{0.8}Mn_{0.2}O_{3-\delta}$ electrode scaffold-type micro tubular solid oxide fuel cells by electrophoretic deposition

Sang-Hoon Lee[a] and Ki-Tae Lee[a,b,*]

[a]*Division of Advanced Materials Engineering, Chonbuk National University Jeonbuk 560-756, Korea*
[b]*Hydrogen and Fuel Cell Research Center, Chonbuk National University, Jeonbuk, 561-756 Korea*

Symmetrical $La_{0.7}Ca_{0.3}Cr_{0.8}Mn_{0.2}O_{3-\delta}$ (LCCM) electrode scaffold-type microtubular solid oxide fuel cells (SOFC) with yttria-stabilized zirconia (YSZ) were fabricated via electrophoretic deposition (EPD). Multi-layers of the LCCM-YSZ anode, an YSZ electrolyte, and an LCCM-YSZ cathode were deposited in consecutive order on a graphite rod via EPD. Since both the cathode and anode were used with the same material, a single cell could be obtained by a one-step co-firing processing. While electrical conductivity increased with the amount of phosphate ester (PE) as a charging agent, the pH decreased. The thickness of the YSZ electrolyte layer increased with the applied voltage and deposition time. The maximum power density of the symmetrical microtubular SOFC single cells with the configuration of LCCM-YSZ anode//YSZ electrolyte//LCCM-YSZ cathode was 106 and 141 mW/cm^2 at 500 and 600 ^{o}C, respectively. After the 10th redox cycle, the single cell exhibited no significant performance degradation.

Key words: Solid oxide fuel cells, Micro tubular, Electrophoretic deposition,s Symmetrical electrode, Scaffold.

Introduction

Solid oxide fuel cells (SOFCs) have the highest energy conversion efficiency among various fuel cell types [1-3]. SOFCs can be divided into two categories according to their cell design: planar and tubular type. Tubular SOFCs have many advantages in terms of their good mechanical strength, easy sealing, and a simple stacking process [4, 5]. Meanwhile, electrophoretic deposition (EPD) is a very useful technique for depositing thin or thick layers due to the ease of layer thickness control by voltage and time [6, 7]. When a dc electric field is applied to the carbon rod in the slurry, the charging agent carries the particles to a substrate. One of the major advantages of EPD is to fabricate a multi-layer structure with a complicated configuration at the same time. Therefore, EPD is a suitable process for the fabrication of tubular SOFC. Although EPD can reduce the steps of SOFC single cell fabrication compared to the conventional process, several steps are still needed because different materials are used for different types of electrodes. For example, cathodes and anodes typically need to be sintered by separate processes. Therefore, the use of a symmetrical electrode reduces the number of EPD process steps as well as the preparation of electrode slurries. However, when a symmetrical electrode is used in both oxidizing and reducing atmospheres, the electrode material should have a high enough electrical conductivity and catalytic activity in both the cathode and anode sides [8-13].

$La_{0.7}Ca_{0.3}Cr_{0.8}Mn_{0.2}O_{3-\delta}$ (LCCM) is considered a promising symmetrical electrode material because it is very stable and exhibits high catalytic activity in both oxidizing and reducing atmospheres [12]. Therefore, it can be used as an electrode material that can complement the symmetrical yttria-stabilized zirconia (YSZ) scaffold electrode. However, the sintering temperature of LCCM is approximately 1200 ^{o}C, while the sintering temperature of conventional electrolytes such as YSZ and $La_{0.8}Sr_{0.2}Ga_{0.8}Mg_{0.2}O_{3-\delta}$ (LSGM) is generally greater than 1450 ^{o}C [14-16]. Considering this sintering property, a symmetrical electrode should be formed as a composite of LCCM-YSZ.

In this study, symmetrical microtubular SOFC single cells with the configuration of LCCM-YSZ anode// YSZ electrolyte//LCCM-YSZ cathode were fabricated via EPD. The dependence of the property and performance on various processing conditions, such as the amount of charging agent, applied voltage, and deposition time, were investigated.

Experimental Procedure

$La_{0.7}Ca_{0.3}Cr_{0.8}Mn_{0.2}O_{3-\delta}$ (LCCM) powder was synthesized by a glycine-nitrate process (GNP) method [12]. As-synthesized LCCM powder was mixed with 40 vol.% YSZ. In order to prepare the slurry of the electrode layer, LCCM-YSZ composite powders were ball-milled with 30 wt.% polymethyl methacrylate (PMMA,

*Corresponding author:
Tel : +82-63-270-2290
Fax: +82-63-270-2386
E-mail: ktlee71@jbnu.ac.kr

SUNPMMA-S100, Sunjin Chem, Korea) as a pore former, 2.5 wt.% polyvinyl butyral (PVB, Aldrich) as a binder, various amounts of phosphate ester (PE, ethyl acid phosphate, Johoku Chem, Japan) as a dispersant, and 200 ml anhydrous ethanol as an organic solvent. Electrolyte material was used with commercial YSZ powder (TZ-8YS, Tosoh, Japan). The slurry of the electrolyte layer was prepared by mixing the YSZ powder, PVB, and anhydrous ethanol without PMMA.

All components of the slurries were thoroughly mixed by ball-milling for 15 h. The prepared stable slurries for the LCCM-YSZ anode layer, YSZ electrolyte layer, and LCCM-YSZ cathode layer were deposited sequentially on a graphite rod (Alfa Aesar, graphite rod, 3-mm diameter) with a constant current, various voltages, and various times. The deposited graphite rod was sintered at 1400 °C for 5 h in air.

Gold paste as a current collector was evenly applied to both the anode and cathode sides of the single cell, which was then fired at 800 °C for 1 h. Current-voltage (I-V) measurements of the single cells were performed using a fuel cell test station (SMART2, WonATech Co. Ltd, Korea) at 500 and 600 °C. Humidified H_2 (~3% H_2O at 30 °C) and dry air were supplied as a fuel and oxidant at flow rates of 30 and 100 cm^3/min, respectively.

Results and Discussion

The first step of EPD is the preparation of a stable slurry for each coating layer. Stability without sedimentation for a long time and a sufficient driving force for moving the particles in the slurry should be considered for the slurry preparation. In this regard, the pH and electrical conductivity of the slurries for electrode and electrolyte layers were investigated according to the PE concentration, as shown in Fig. 1. While electrical conductivity gradually increased with the amount of PE, the pH decreased. When PE is dissociated in organic solvent, the hydroxyl group from the organic solvent combines the dissociated PE and release protons. Therefore, the electrical conductivity increases, but the pH decreases with the PE concentration due to an increase in the amount of the released protons. Although a high electrical conductivity is needed to provide enough mobility of particles in the slurry, there is a trade-off between the electrical conductivity and stability related to the pH. The optimal conditions for the slurry of the LCCM-YSZ anode and YSZ electrolyte layers are listed in Table 1.

Upon optimizing the slurries, the LCCM-YSZ anode layer, YSZ electrolyte layer, and LCCM-YSZ cathode layer were deposited consecutively on a graphite rod. In order to verify the correlation between the microstructure and deposition conditions, the YSZ electrolyte layer was deposited with various deposition times and voltages. Fig. 2 shows the microstructure of multi-layers co-fired at 1400 °C for 5 h after deposition

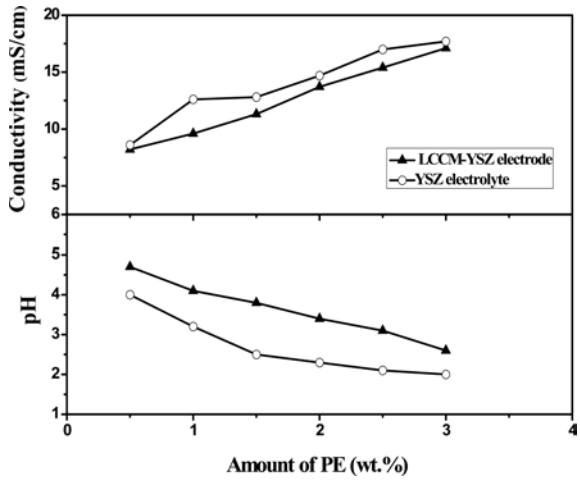

Fig. 1. Conductivity and pH of the LCCM-YSZ electrode layer and YSZ electrolyte layer slurries as a function of PE concentration.

Table 1. Optimal slurry conditions for the EPD process.

Slurry	PE (wt%)	PVB (wt%)	PMMA (vol%)	Solid loading (solute: solvent)
LCCM-YSZ	0.5	2.5	30	25:100
YSZ electrolyte	0.5	2.5	–	20:100

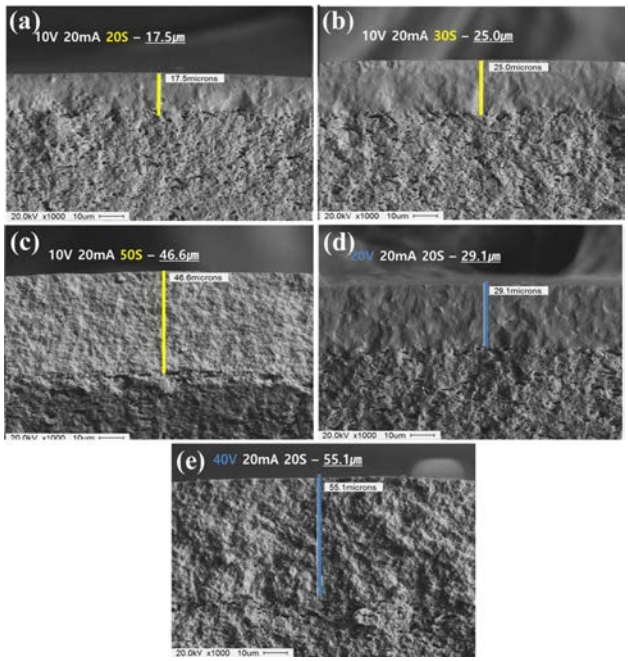

Fig. 2. Cross-sectional SEM images of the YSZ electrolyte deposited with various parameters: (a) 10 V and 20 s, (b) 10 V and 30 s, (c) 10 V and 50 s, (d) 20 V and 20 s, and (e) 40 V and 20 s.

at various times and voltages. The thickness of the YSZ electrolyte layer gradually increased as the deposition time increased at the same voltage and current (10 V, 20 mA) as shown in Figs. 2(a), (b), and

Table 2. Optimal deposition conditions for the EPD process.

Layer	Voltage (V)	Current (mA)	Time (s)
LCCM-YSZ anode	40	20	60
YSZ electrolyte	20	20	20
LCCM-YSZ cathode	20	20	20

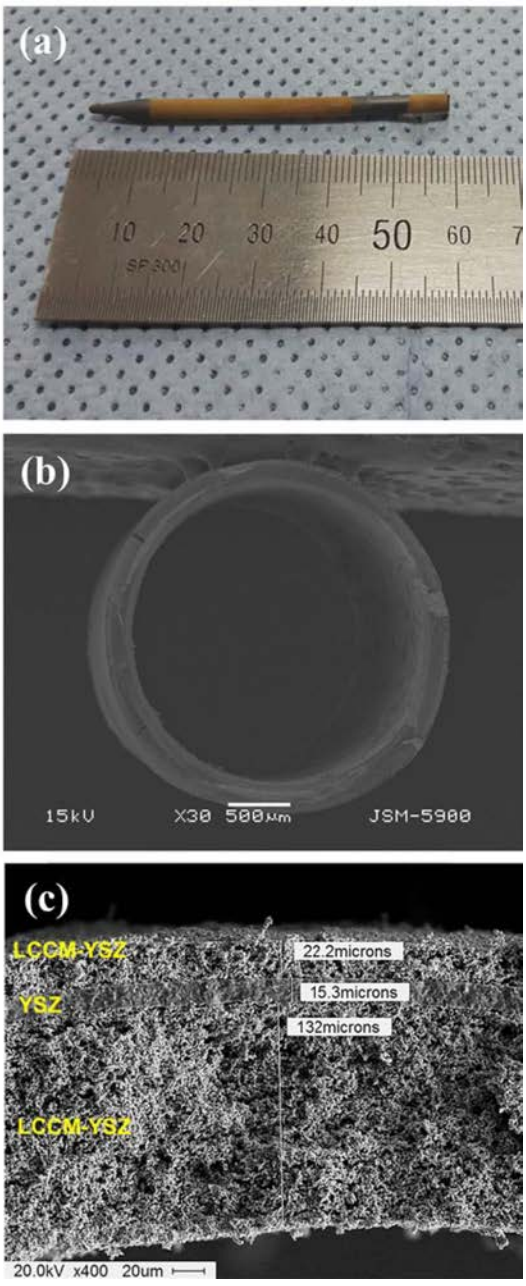

Fig. 3. The picture and cross-sectional SEM image of the microtubular SOFC single cell with the configuration of LCCM-YSZ anode//YSZ electrolyte//LCCM-YSZ cathode that was fabricated by the EPD process.

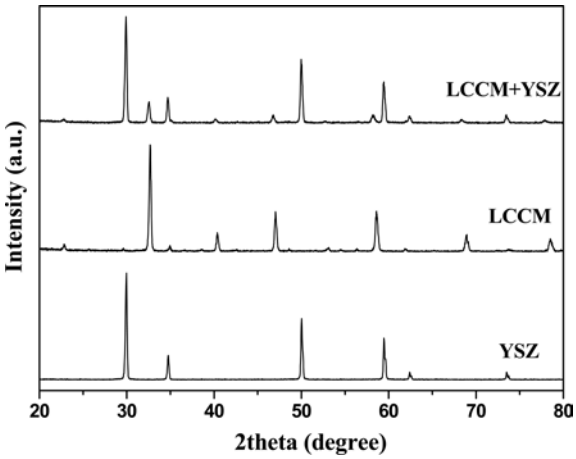

Fig. 4. XRD patterns of the mixture of LCCM and YSZ fired at 1400 °C for 5 h in air.

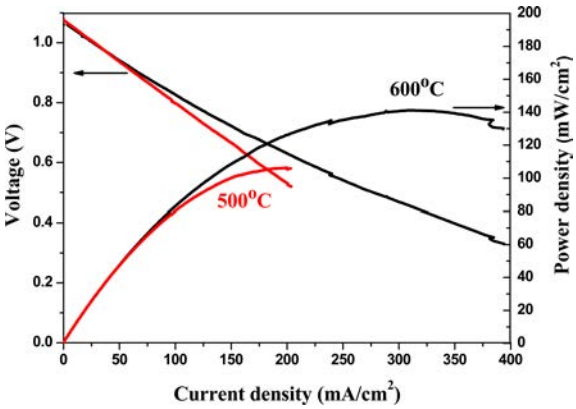

Fig. 5. Current-voltage (I-V) and power density curves for the symmetrical microtubular SOFC single cells with the configuration of LCCM-YSZ anode//YSZ electrolyte//LCCM-YSZ cathode fabricated by the EPD process and measured at 500 and 600 °C.

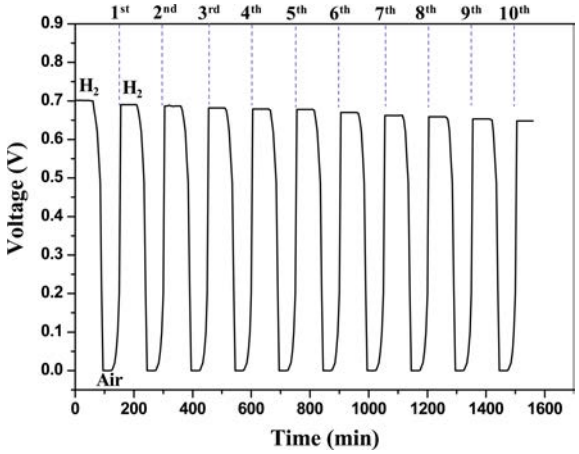

Fig. 6. Redox stability of the symmetrical microtubular SOFC single cells with the LCCM-YSZ anode//YSZ electrolyte//LCCM-YSZ cathode fabricated by the EPD process.

(c). At the same deposition time and current (20 s, 20 mA), the thickness also increased with an increase in voltage, as shown in Figs. 2(a), (d), and (e). These results indicate that the thin film thickness can be precisely controlled through proper adjustments of the deposition parameters such as voltage and deposition

time. The optimal deposition conditions for the LCCM-YSZ anode layer, YSZ electrolyte layer, and LCCM-YSZ cathode layer to produce crack-free rigid symmetrical microtubular SOFC single cells are listed in Table 2.

Fig. 3 shows the picture and microstructure of the fabricated symmetrical microtubular SOFC single cell with a 2.75 mm diameter and 58 mm length after sintering at 1400 °C for 5 h in air. The thick inner layer of the LCCM-YSZ anode acts as a support to sustain the single cell. All fabricated layers were well attached with no delamination or cracks. In particular, the thin YSZ electrolyte was very dense without any pinholes. The effective electrode area was 2.85 cm^2.

Additionally, a high temperature co-firing step is one of the essential processes for fabricating the symmetrical microtubular SOFC single cells via the EPD process. However, a high sintering temperature may cause serious problems such as the reaction between the attached layers leading to performance degradation and single cell destruction. Therefore, in order to confirm the reaction between LCCM and YSZ, the mixture of LCCM and YSZ was fired at 1400 °C for 5 h and then analyzed via X-ray diffraction (XRD). As shown in Fig. 4, no secondary phase was detected, which indicates that LCCM and YSZ do not react during high-temperature sintering at 1400 °C for 5 h.

The cell voltages and power densities of symmetrical microtubular SOFC single cells with the configuration of LCCM-YSZ anode//YSZ electrolyte//LCCM-YSZ cathode at 500 and 600 °C are shown in Fig. 5. The open circuit voltage values at 500 and 600 °C were 1.08 and 1.06 V, respectively, which indicates that the microtubular single cells with very thin electrolyte can maintain tight sealing without sealant. The maximum power density was 106 and 141 mW/cm^2 at 500 and 600 °C, respectively. Such results represent a considerable electrochemical performance when compared to that of conventional YSZ electrolyte-based single cells.

Redox cycle test results are shown in Fig. 6. In one redox cycle, a single cell operating on a constant current load of 160 mA/cm^2 at 600 °C with H_2 fuel for 1 h and air was flowing for 30 min instead of H_2. N_2 gas was purged for 30 min between H_2 and air flow. After 10 cycles, the single cell showed no significant performance degradation.

Conclusions

A main advantage of EPD is the ability to prepare green bodies of multi-layered microtubular SOFC single cells in one batch process within several minutes. The final microstructure of single cells, such as the thickness of thin or thick film, can be precisely controlled by changing the conditions of the slurry and the deposition parameters. In order to maximize the advantage of EPD, we proposed symmetrical microtubular SOFC single cells with the configuration of the LCCM-YSZ anode//YSZ electrolyte//LCCM-YSZ cathode in this study. Unlike conventional SOFC single cells in which the anode and cathode should be fired separately due to their significantly different sintering temperatures, a symmetrical microtubular SOFC single cell can be obtained by one-step co-firing processing. Moreover, the symmetrical LCCM electrode-based, scaffold-type microtubular SOFC single cell fabricated via EPD exhibited considerable electrochemical performance.

Acknowledgments

This work was supported by the Technology Development Program to Solve Climate Changes of the National Research Foundation (NRF) grant funded by the Korea government (Ministry of Science and ICT) (2017M1A2A2044930). This work was also supported by the Korea Institute of Energy Technology Evaluation and Planning (KETEP) and the Ministry of Trade, Industry & Energy (MOTIE) of the Republic of Korea (No. 20164030201070).

References

1. N.Q. Minh, J. Am. Ceram. Soc. 76 (1993) 563.
2. B.C.H. Steele, A. Heinzel, Nature 41(2001) 345.
3. S.C. Singhal, K. Kendall, High Temperature Solid Oxide Fuel Cells, Elsevier, 2003.
4. H. Kim, W.J. Kim, J.W. Lee, S.B. Lee, T.H. Lim, S.J. Park, R.H. Song, D.R. Shin, Kor. J. Chem. Eng. 50 [4] (2012) 749.
5. J.S. Cherng, C.C Wu, F.A. Yu, T.H. Yeh, J. Power Sources 232 (2013) 353.
6. P. Sarkar, J. Mater. Sci. 39 (2004) 819.
7. O.O. Van Der Biest, L.J. Vandeperre, J. Mater. Sc. 29 (1999) 325.
8. Y. Wang, T. Liu, S. Fang, F. Chen, J. Power Sources, 305 (2016) 240-248.
9. C. Su, W. Wang, M. Liu, M.O. Tade, Z. Shao, Adv. Energy Mater., 5 (2015) 1-19.
10. W. Tan, C. Pan, S. Yang, Q. Zhong, J. Power Sources, 277 (2015) 416-425.
11. Z. Yang, Y. Chen, C. Jin, G. Xiao, M. Han, F. Chen, RSC Advances, 5 (2015) 2702-2705.
12. M.K. Rath, K.T. Lee, Ceram. Int., 41 (2015) 10878-10890.
13. M.K. Rath, K.T. Lee, Electrochim. Acta, 212 (2016) 678-685.
14. K. Yin, Z.D. Cui, X.R. Zheng, X.J. Yang, S.L. Zhu, Z.Y. Li, Y.Q. Liang, J. Mater. Chem. A, 3 (2015) 22770-22780.
15. A. Buyukaksoy, S.P. Kammampata, V.I. Birss, J. Power Sources, 287 (2015) 349-358.
16. K.J. Kim, S.W. Choi, M.Y. Kim, M.S. Lee, Y.S. Kim, H.S. Kim, J. Ind.Eng. Chem., 42 (2016) 69-74.